

# The Directional Transport of Self-Propelled Ellipsoidal Particles Confined in 2D Channel

Bing Wang\*, Zhongwei Qu, Xuechao Li

Department of Physics and Mathematics, Anhui University of Science and Technology, Huainan, 232001, P.R.China

**Abstract:** Directional transport of self-propelled ellipsoidal particles confined in a smooth corrugated channel with a asymmetric potential and Gaussian colored noise is investigated. Effects of the channel, potential and coloured noise are discussed. The moving direction changes from in  $+x$  direction to in  $-x$  direction with increasing load  $f$ . Proper size of the pore is good for the directional transport, but too large or too small pore size will inhibit this phenomenon. Large  $x$  axis noise intensity will inhibit the transport in  $-x$  and  $+x$  direction. But the directional transport speed  $|\langle V \rangle|$  has a maximum with increasing  $y$  axis noise intensity. Transport reverse phenomenon will appear with increasing self-propelled speed  $v_0$ . Perfect sphere particle is more easier for directional transport than needlelike ellipsoid particle.

**Keywords:** Self-propelled Ellipsoidal Particle; Confined Channel; Directional Transport

## 1 Introduction

Recent years, we have seen enormous activities, both theoretical and experimental, in the study of the properties of the confined particles. These studies found spatial confinement can fundamentally change equilibrium and dynamical properties of a system via two different effects: limiting the configuration space accessible to its diffusing components[1] and increasing the hydrodynamic drag on them[2]. There exists a large variety of natural and artificial confined geometries, e.g., biological cells[3], zeolites[4], artificial nanopores[5, 6], ionpumps[7, 9] and micro fluidic devices[10–13].

Confined particle shows a series of novel features, e.g. current reversal[14, 15], self-organization[16, 17], geometry-induced stochastic resonance[18, 19] and so on. Hänggi *et al.* proposed a simple scheme for absolute negative mobility(A device is said to operate in the absolute negative mobility regime, when it works steadily against a biased force.) of asymmetry particle in a compartmentalized channel or a rough channel[20]. Using molecular dynamics simulations, Sobrino Fernandez *et al.* studied the self-assembly phenomenon of Janus particles when confined in a channel.[21]. Ghosh *et al.* investigated self-propelled over damped microswimmers in a two dimensional periodically compartmentalized channel and proved that ratcheting of Janus particles can be orders of magnitude stronger than for ordinary thermal potential ratchets[22]. Liu *et al.* investigated the self-propelled Janus particles moves in a double cavity container and found the entropic stochastic resonance can survive even if there is no symmetry breaking in any direction[23]. Pu *et al.* investigated the reentrant phase separation behavior of active particles with anisotropic Janus interaction and found that phase separation shows a re-entrance behavior with variation of the Janus interaction strength[24]. Xu *et al.* studied the effects of ion channel blocks on electrical activity of stochastic Hodgkin-Huxley neural network under electromagnetic induction[25]. Ai *et al.* investigated the rectified transport of active ellipsoidal particles in a two-dimensional asymmetric potential[26].

Traditionally, stochastic differential equations used in physical and biological science have involved Gaussian white noise. Laser noise problems [27, 28], bistable system[29, 30] and self-propelled particle

---

\*Corresponding author.Email:hnitwb@163.com

system[31, 32] have been shown to necessitate the use of coloured noise instead of white noise.

In this paper, we investigate the transport phenomenon of self-propelled ellipsoidal Brownian particles confined in a two dimensional(2D) smooth channel. The paper is organized as follows: In Sect.2, the basic model of confined self-propelled ellipsoidal particles with coloured noise is provided. In Sect.3, the effects of parameters are investigated by means of simulations. In Sect. 4, we get the conclusions.

## 2 Basic model and methods

In this work, we consider self-propelled ellipsoidal particles confined in a 2D smooth corrugated channel with a two-dimensional asymmetric potential and coloured noises. In the lab frame, the particle's displacement  $\delta\vec{R}(t)$  can be described by its mass center( $\delta x, \delta y$ ). The dynamics of the particle can be described by the following Langevin equations[26]

$$\frac{\partial x}{\partial t} = v_0 \cos \theta(t) + F_x[\bar{\Gamma} + \Delta\Gamma \cos 2\theta(t)] + \Delta\Gamma F_y \sin 2\theta(t) + \xi_x(t), \quad (1)$$

$$\frac{\partial y}{\partial t} = v_0 \sin \theta(t) + F_y[\bar{\Gamma} - \Delta\Gamma \cos 2\theta(t)] + \Delta\Gamma F_x \sin 2\theta(t) + \xi_y(t), \quad (2)$$

$$\frac{\partial \theta(t)}{\partial t} = \Gamma_\theta \tau + \xi_\theta(t). \quad (3)$$

The angle between the lab frame  $x$  axis and the body frame  $\hat{x}$  axis is  $\theta(t)$ .  $v_0$  is the self-propelled velocity and along the long axis of the particle. The quantities  $\bar{\Gamma} = \frac{1}{2}(\Gamma_x + \Gamma_y)$  and  $\Delta\Gamma = \frac{1}{2}(\Gamma_x - \Gamma_y)$  are the average and difference mobilities of the body, respectively. The mobilities along its long axis and short axis and are  $\Gamma_x$  and  $\Gamma_y$ , respectively. The rotational mobility is  $\Gamma_\theta$ . The parameter  $\Delta\Gamma$  determines the asymmetry of the body. The particle is a perfect sphere for  $\Delta\Gamma = 0$  and a very needlelike ellipsoid for  $\Delta\Gamma \rightarrow \bar{\Gamma}$ . The torque  $\tau$  acting on the body due to its orientation relative to the direction of the potential field. The noises  $\xi_x$  and  $\xi_y$  parallel to  $x$  axis and  $y$  axis, respectively(If the particle is a charged particle,  $\xi_x$  and  $\xi_y$  can be seen as electric-field noises with different intensities and self-correlation times[33, 34]). The noises  $\xi_x, \xi_y$  and  $\xi_\theta$  satisfy the following relations,

$$\langle \xi_i(t) \rangle = 0, (i = x, y, \theta), \quad (4)$$

$$\langle \xi_i(t) \xi_j(t') \rangle = \delta_{ij} \frac{Q_i}{\tau_i} \exp[-\frac{|t-t'|}{\tau_i}], (i = x, y, \theta). \quad (5)$$

$\langle \dots \rangle$  denotes an ensemble average over the distribution of the random forces.  $Q_i$  is the noise intensity.  $\tau_i$  is the self-correlation time.

The particles are confined in a two dimensional smooth corrugated channel. The channel is consisted of many cavities. And the channel is periodic in space along the  $x$ -axis as shown in Fig.1. The walls of the cavity are been modeled by the following sinusoidal functions[35]

$$W_+(x) = \frac{1}{2}[\Delta + (y_L - \Delta) \sin^\eta(\frac{\pi x}{x_L})], \quad (6)$$

$$W_-(x) = -\frac{1}{2}[\Delta + (y_L - \Delta) \sin^\eta(\frac{\pi x}{x_L})], \quad (7)$$

where  $x_L = 1.0$  and  $y_L = 1.0$  are the length and width of the cavity, respectively. The additional tunable geometric parameter is  $\eta$ . For  $\eta = 2$ , the cavity represents the compartment of sinusoidally corrugated channel. When  $\eta \rightarrow 0$ , the cavity reproduces the compartment of sharply corrugated channels. The channel width is  $h(x) = W_+ - W_-$ . The minimal channel width(the pore) is  $h_{min} = h(x)|_{x=\pm k, k=0,1,2,\dots} = \Delta$ , and through which the particles can exit the cavity. The maximal channel width is  $h_{max} = h(x)|_{x=\pm(2k+1)\frac{1}{2}, k=0,1,2,\dots} = y_L$ .

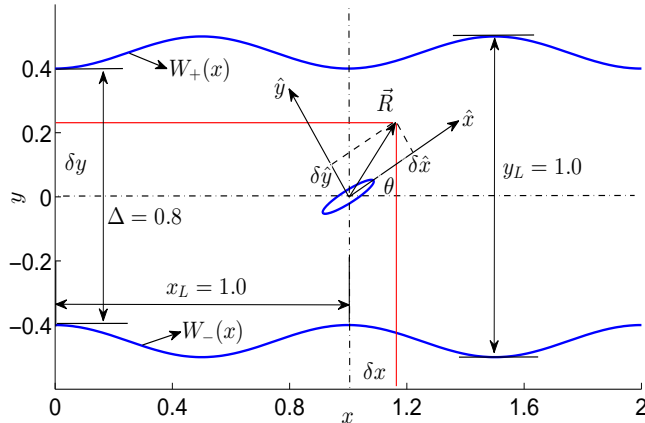


Figure 1: Illustrations of the smooth corrugated channel with  $\Delta = 0.8$ ,  $x_L = y_L = 1.0$ ,  $\eta = 2.0$ .

The forces  $F_x$  and  $F_y$  are along  $x$  and  $y$  directions of the lab frame, respectively.  $F_x = -\frac{\partial U}{\partial x}$  and  $F_y = -\frac{\partial U}{\partial y}$ . We consider the following asymmetric potential[36](shown in Fig.2),

$$U(x, y) = \frac{U_0}{2}y^2[\cos(x + \varepsilon \ln \cosh y) + 1.1] + fx. \quad (8)$$

Here,  $U_0$  is the height of the potential and  $f$  is the load. The asymmetric parameter of the potential is  $\varepsilon$ , and the potential is symmetric for  $\varepsilon = 0.0$ . The equipotential is look like a herringbone pattern for  $\varepsilon \neq 0$ .

A central practical question in the theory of Brownian motors is the over all long time behavior of the particle, and the key quantities of particle transport is the particle velocity. Because the channel along  $y$  direction are confined, we only calculate the  $x$  direction average velocity

$$\langle V_{\theta_0} \rangle = \lim_{t \rightarrow \infty} \frac{\langle x(t) - x(t_0) \rangle}{t - t_0}, \quad (9)$$

the position of particles at time  $t_0$  is  $x(t_0)$ . The initial angle of the trajectory is  $\theta_0$ . The full average velocity after another average over all  $\theta_0$  is

$$\langle V \rangle = \frac{1}{2\pi} \int_0^{2\pi} \langle V_{\theta_0} \rangle d\theta_0. \quad (10)$$

### 3 Results and discussion

In this letter, we demonstrate the properties of self-propelled ellipsoidal particles confined in the  $2D$  smooth corrugated channel. In order to give a simple and clear analysis of the system. Eqs.(1,2,3) are integrated using the Euler algorithm. The integration step time  $\Delta t = 10^{-4}$  and the stochastic averages are obtained as ensemble averages over  $10^5$  trajectories with random initial conditions. In the simulation, we set  $x_L = y_L = 1.0$ ,  $\bar{\Gamma} = 1.0$ ,  $U_0 = 1.0$  and  $\tau = 0.0$  throughout the paper. As  $\tau$  is the torque acting on the particle. So the particle is independent of external torque in this paper.

The average velocity  $\langle V \rangle$  as a function of the load  $f$  for different  $\eta$  is reported in Fig.3. We find  $\langle V \rangle$  decreases monotonically with increasing load  $f$ .  $\langle V \rangle > 0$  when  $f < 0$ , but  $\langle V \rangle < 0$  when  $f > 0$ . This means negative load will lead to positive transport, but positive load will lead to negative transport. Directional transport speed  $\langle V \rangle$  increases with increasing  $|f|$ , so large load  $|f|$ (in  $x$  direction or in  $-x$  direction) is good for directional transport(in  $x$  direction or in  $-x$  direction). We know the potential  $U$

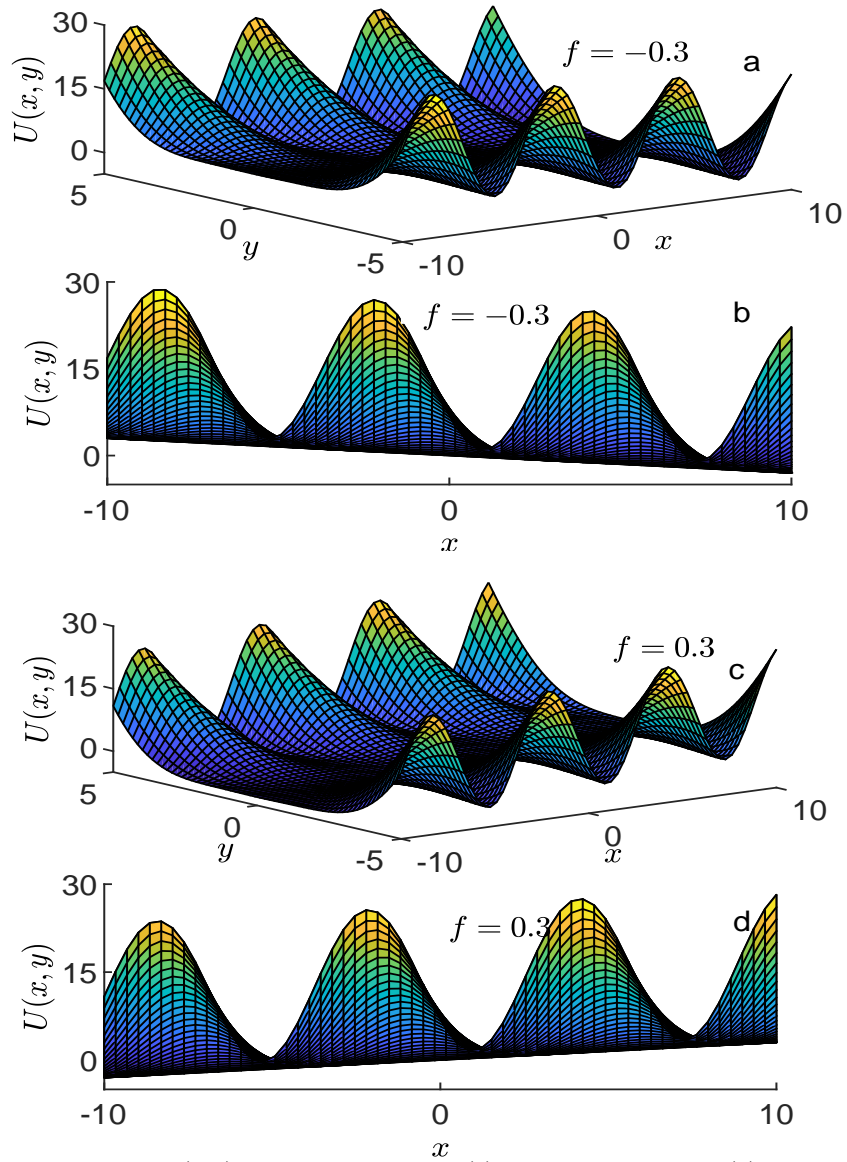


Figure 2: The asymmetric potential  $U(x, y)$  with  $U_0 = 1.0$ ,  $\varepsilon = 0.5$ :(a)3D view with  $f = -0.3$ ;(b)Front view with  $f = -0.3$ ;(c)3D view with  $f = 0.3$ ;(d)Front view with  $f = 0.3$ .

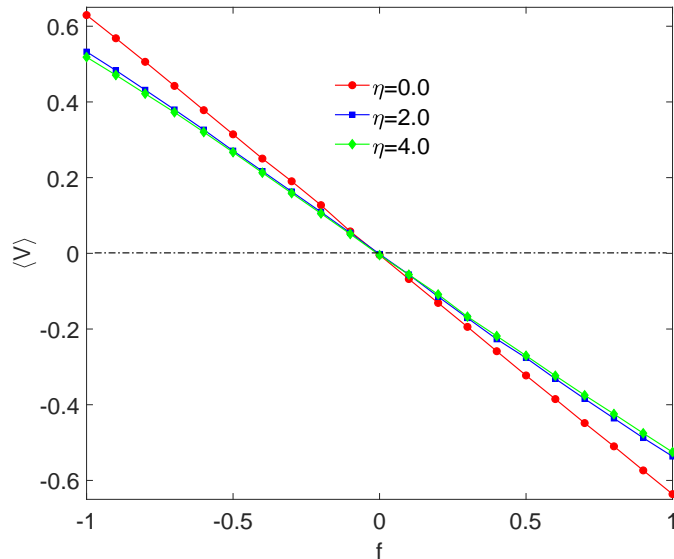


Figure 3: The average velocity  $\langle V \rangle$  as a function of load  $f$  for different  $\eta$ . The other parameters are  $\Delta = 0.8$ ,  $\varepsilon = 0.5$ ,  $v_0 = 0.5$ ,  $Q_x = Q_y = Q_\theta = 1.0$ ,  $\tau_x = \tau_y = \tau_\theta = 1.0$ .

is inversely proportional to the load  $f$ (Fig.2), so the particle moves to the place where potential is lower. In this figure, we find the smaller  $\eta$ , the larger  $|\langle V \rangle|$  is.

The average velocity  $\langle V \rangle$  as a function of the pore size(the minimal channel width)  $\Delta$  is reported in Fig.4. We find  $\langle V \rangle \rightarrow 0$  when  $\Delta \rightarrow 0$ . The directional transport speed  $|\langle V \rangle|$  increases with increasing  $\Delta$ , and reaches a maximum when  $\Delta = 1$ , then decreases with increasing  $\Delta$ . We know the narrower the pore is, the more difficult of the particles exit the cavity(or directional transport). So an interesting phenomena appears, that is, too large pore size instead of help to the particle directional transport, but restrain this directional transport phenomenon.

The average velocity  $\langle V \rangle$  as a function of self-propelled speed  $v_0$  with different  $f$  is reported in Fig.5. When the load is negative( $f = -0.3$  and  $f = -0.1$ ), inert particle(self-propelled speed  $v_0 = 0$ ) moves along  $+x$  direction( $\langle V \rangle > 0$ ), and  $\langle V \rangle$  decreases with increasing  $v_0$ , then the moving direction changes to  $-x$  direction when  $2.8 < v_0 < 6.0$ , and  $\langle V \rangle \rightarrow 0$  when  $v_0 = 6.0$ . When the load is positive( $f = 0.1$  and  $f = 0.3$ ), inert particle moves in  $-x$  direction( $\langle V \rangle < 0$ ), and with increasing  $v_0$ , the transport reverse phenomenon appears too, and  $\langle V \rangle \rightarrow 0$  when  $v_0 = 6.0$ .

The average velocity  $\langle V \rangle$  as a function of the asymmetry of the body  $\Delta\Gamma$  for different  $f$  is reported in Fig.6. We know  $\Delta\Gamma$  characterizes the asymmetry of the particle, and the particle is a perfect sphere when  $\Delta\Gamma = 0$ , the particle is a very needlelike ellipsoid when  $\Delta\Gamma \rightarrow \bar{\Gamma}$ . In this figure, we find the directional transport speed  $|\langle V \rangle|$  decreases with increasing  $\Delta\Gamma$ . So perfect sphere particle is more easier for directional transport than needlelike ellipsoid particle.

The average velocity  $\langle V \rangle$  as a function of  $x$  axis noise intensity  $Q_x$  for different load  $f$  is reported in Fig.7. We find the directional transport speed  $|\langle V \rangle|$  decreases with increasing  $Q_x$ , so large  $x$  axis noise intensity will inhibit  $x$  directional transport.

The average velocity  $\langle V \rangle$  as a function of self-correlation time  $\tau_x$  for different load  $f$  is reported in Fig.8. In this figure, compare with the effect of  $x$  axis noise intensity, we find  $\tau_x$  has exactly the reverse effect on the system. The directional transport speed  $|\langle V \rangle|$  increases with increasing  $\tau_x$ , so large self-correlation time  $\tau_x$  is good for the  $x$  directional transport. From Figs. 7 and 8, we find the slopes of  $\langle V \rangle - Q_x$  and  $\langle V \rangle - \tau_x$  curves almost changes to zero when  $Q_x$  and  $\tau_x$  are large. So changes of  $Q_x$  and  $\tau_x$  have weak impact on the directional transport when their values are large.

The average velocity  $\langle V \rangle$  as a function of  $y$  axis noise intensity  $Q_y$  for different  $f$  is reported in Fig.9. In this figure, we find the directional transport speed  $|\langle V \rangle|$  has a maximum with increasing  $Q_y$ . So proper

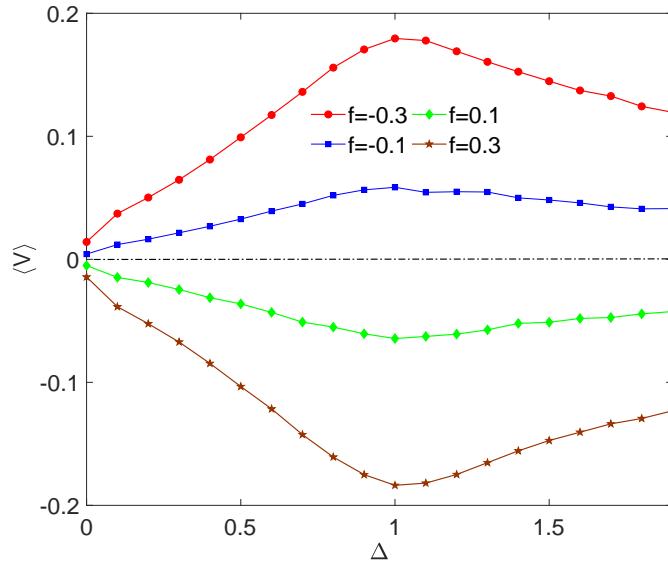


Figure 4: The average velocity  $\langle V \rangle$  as a function of pore size  $\Delta$  for different values of  $f$ . The other parameters are  $\varepsilon = 0.5$ ,  $\eta = 2.0$ ,  $v_0 = 0.5$ ,  $Q_x = Q_y = Q_\theta = 1.0$ ,  $\tau_x = \tau_y = \tau_\theta = 1.0$ .

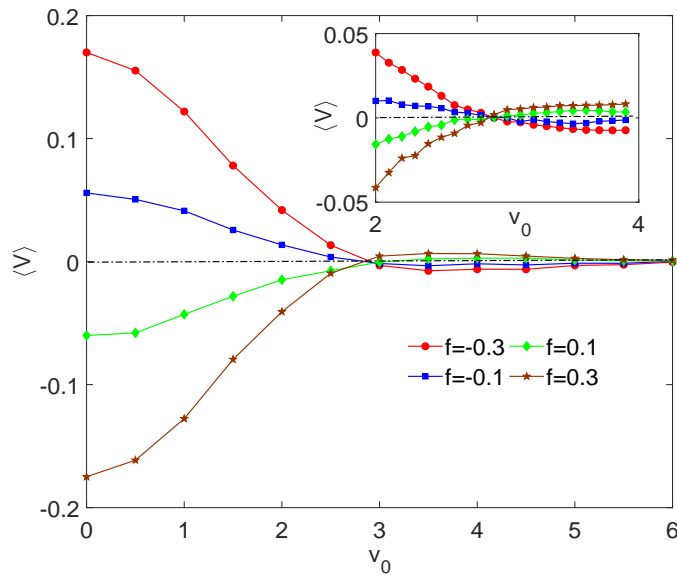


Figure 5: The average velocity  $\langle V \rangle$  as a function of self-propelled speed  $v_0$  for different values of  $f$ . The other parameters are  $\Delta = 0.8$ ,  $\varepsilon = 0.5$ ,  $\eta = 2.0$ ,  $Q_x = Q_y = Q_\theta = 1.0$ ,  $\tau_x = \tau_y = \tau_\theta = 1.0$ .

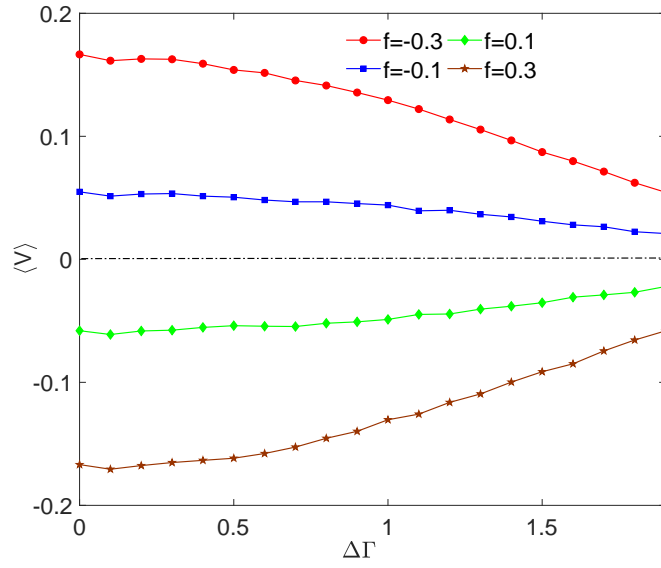


Figure 6: The average velocity  $\langle V \rangle$  as a function of  $\Delta\Gamma$  for different values of  $f$ . The other parameters are  $\Delta = 0.8$ ,  $\varepsilon = 0.5$ ,  $\eta = 2.0$ ,  $v_0 = 0.5$ ,  $Q_x = Q_y = Q_\theta = 1.0$ ,  $\tau_x = \tau_y = \tau_\theta = 1.0$ .

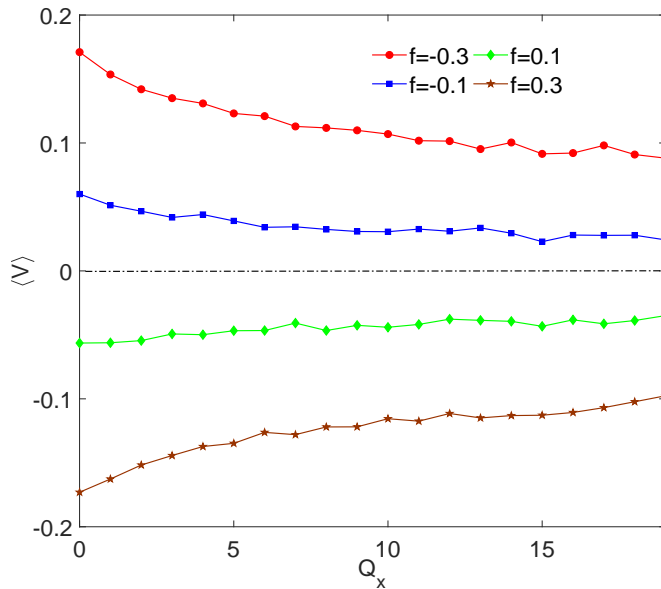


Figure 7: The average velocity  $\langle V \rangle$  as a function of  $Q_x$  for different values of  $f$ . The other parameters are  $\Delta = 0.8$ ,  $\varepsilon = 0.5$ ,  $\eta = 2.0$ ,  $v_0 = 0.5$ ,  $Q_x = Q_y = Q_\theta = 1.0$ ,  $\tau_x = \tau_y = \tau_\theta = 1.0$ .

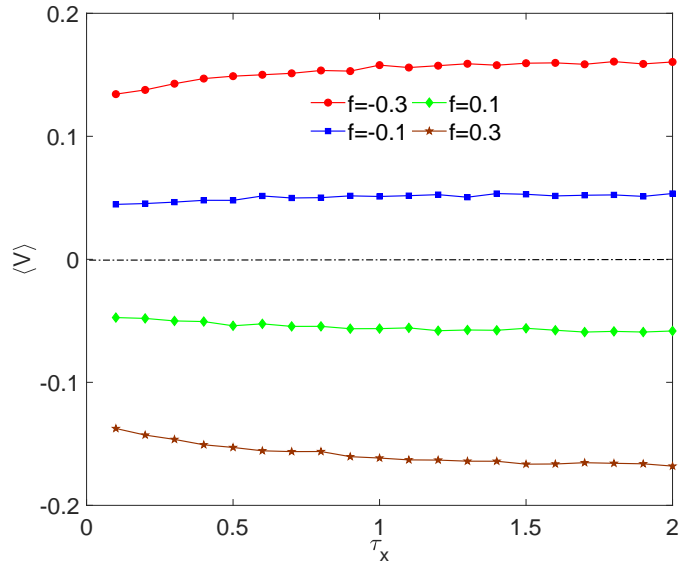


Figure 8: The average velocity  $\langle V \rangle$  as a function of  $\tau_x$  for different values of  $f$ . The other parameters are  $\Delta = 0.8$ ,  $\varepsilon = 0.5$ ,  $\eta = 2.0$ ,  $v_0 = 0.5$ ,  $Q_x = Q_y = Q_\theta = 1.0$ ,  $\tau_y = \tau_\theta = 1.0$ .

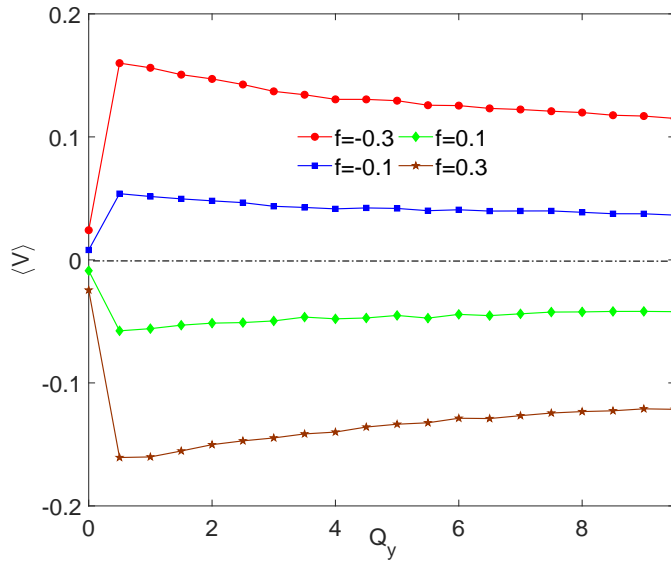


Figure 9: The average velocity  $\langle V \rangle$  as a function of  $Q_y$  for different values of  $f$ . The other parameters are  $\Delta = 0.8$ ,  $\varepsilon = 0.5$ ,  $\eta = 2.0$ ,  $v_0 = 0.5$ ,  $Q_x = Q_\theta = 1.0$ ,  $\tau_x = \tau_y = \tau_\theta = 1.0$ .



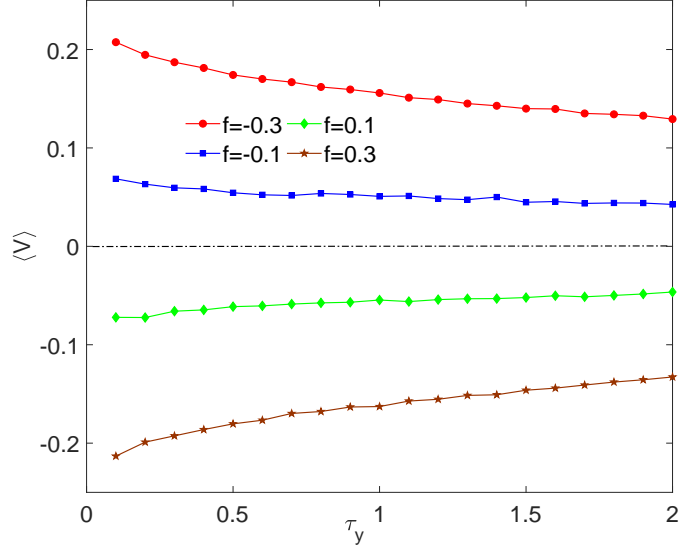


Figure 10: The average velocity  $\langle V \rangle$  as a function of  $\tau_y$  for different values of  $f$ . The other parameters are  $\Delta = 0.8$ ,  $\varepsilon = 0.5$ ,  $\eta = 2.0$ ,  $v_0 = 0.5$ ,  $Q_x = Q_y = Q_\theta = 1.0$ ,  $\tau_x = \tau_\theta = 1.0$ .

$y$  axis noise intensity is good for the  $x$  directional transport, too large or too small  $Q_y$  will inhibit this phenomenon. From figures 7 and 9, we find an interesting phenomenon,  $x$  axis noise intensity will inhibit  $x$  directional transport, but proper  $y$  axis noise intensity is good for this transport.

The average velocity  $\langle V \rangle$  as a function of  $y$  axis noise self-correlation time  $\tau_y$  for different  $f$  is reported in Fig.10. In this figure, compare with the effect of  $x$  component noise self-correlation time  $\tau_x$ , we find large  $\tau_y$  has negative effect on the  $x$  directional transport. The directional transport speed  $|\langle V \rangle|$  decreases with increasing  $\tau_y$ , so large self-correlation time  $\tau_y$  will inhibit the directional transport.

The average velocity  $\langle V \rangle$  as functions of angle noise intensity  $Q_\theta$  and self-correlation time  $\tau_\theta$  for different  $f$  are reported in Figs.11 and 12. In these two figures, we find there will be no changes of  $\langle V \rangle$  with increasing  $Q_\theta$  and  $\tau_\theta$ . So the effect of the angle noise is very weak for the directional transport of the particle.

The average velocity  $\langle V \rangle$  as a function of the asymmetric parameter  $\varepsilon$  for different  $f$  is reported in Fig.13. We find the  $\langle V \rangle - \varepsilon$  curve is almost horizontal, this means that the effect of  $\varepsilon$  is very weakly on the particle directional transport phenomenon.

## 4 Conclusions

In this paper, we numerically investigated the transport phenomenon of self-propelled ellipsoidal particles confined in a two-dimensional smooth channel with coloured noise. We find the moving direction is closely linked to the direction of the load. Negative load will lead to  $x$  directional transport, but positive load will lead to  $-x$  directional transport. Too small and too large pore size will restrain the directional transport of the ellipsoidal particle. Large  $x$  axis noise intensity will inhibit the directional transport. Proper large  $y$  axis noise intensity is good for this phenomenon. Transport reverse phenomenon appears with increasing self-propelled speed  $v_0$ . The effects of angle noise on the system is negligible.

## Acknowledgments

Project supported by Natural Science Foundation of Anhui Province(Grant No:1408085QA11).

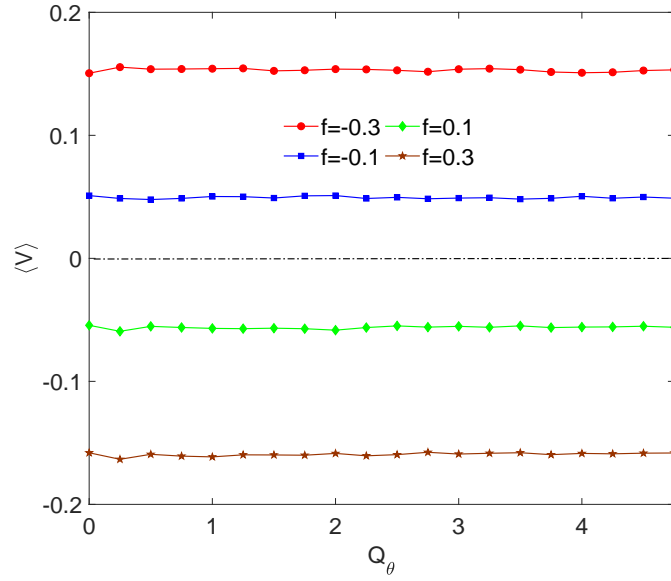


Figure 11: The average velocity  $\langle V \rangle$  as a function of  $Q_\theta$  for different values of  $f$ . The other parameters are  $\Delta = 0.8$ ,  $\varepsilon = 0.5$ ,  $\eta = 2.0$ ,  $v_0 = 0.5$ ,  $Q_x = Q_y = 1.0$ ,  $\tau_x = \tau_y = \tau_\theta = 1.0$ .

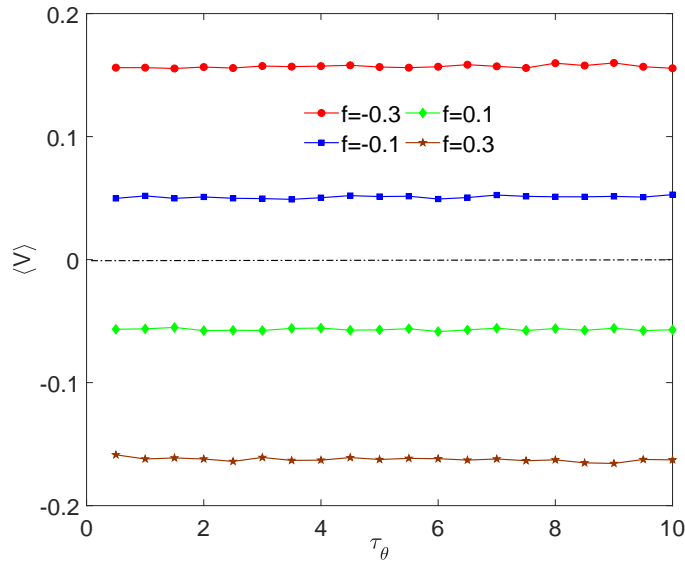


Figure 12: The average velocity  $\langle V \rangle$  as a function of  $\tau_\theta$  for different values of  $f$ . The other parameters are  $\Delta = 0.8$ ,  $\varepsilon = 0.5$ ,  $\eta = 2.0$ ,  $v_0 = 0.5$ ,  $Q_x = Q_y = Q_\theta = 1.0$ ,  $\tau_x = \tau_y = 1.0$ .

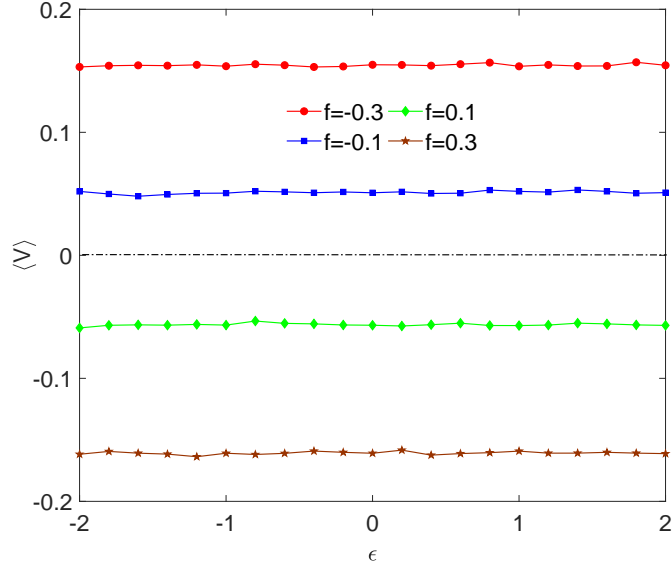


Figure 13: The average velocity  $\langle V \rangle$  as a function of  $\varepsilon$  for different values of  $f$ . The other parameters are  $\Delta = 0.8$ ,  $\eta = 2.0$ ,  $v_0 = 0.5$ ,  $Q_x = Q_y = Q_\theta = 1.0$ ,  $\tau_x = \tau_y = \tau_\theta = 1.0$ .

## References

- [1] P. Hänggi, F. Marchesoni, *Rev. Mod. Phys.* **81** 387 (2009).
- [2] P. S. Burada, P. Hänggi, F. Marchesoni, G. Schmid, P. Talkner, *Chem. Phys. Chem.* **10** 45 (2009).
- [3] H. X. Zhou, G. N. Rivas, A. P. Minton, *Annu. Rev. Biophys.* **37** 375 (2008).
- [4] F. J. Keil, R. Krishna, M. O. Coppens, *Rev. Chem. Eng.* **16** 71 (2000).
- [5] M. Firnkes, D. Pedone, J. Knezevic, M. Döblinger, U. Rant, *Nano. Lett.* **10** 2162 (2010).
- [6] D. Pedone, M. Langecker, G. Abstreiter, U. Rant, *Nano. Lett.* **11** 1561 (2011).
- [7] Z. Siwy, A. Fulinski, *Am. J. Phys.* **72** 567 (2004).
- [8] B. Lindner, J. Garcia-Ojalvo, A. Neiman, L. Schimansky-Geier, *Phys. Rep.* **392** 321 (2004).
- [9] Z. Siwy, I. D. Kosinska, A. Fulinski, C. R. Martin, *Phys. Rev. Lett.* **94** 048102 (2005).
- [10] S. Matthias, F. Müller, *Nature* **424** 53 (2003).
- [11] T. M. Squires, S. R. Quake, *Rev. Mod. Phys.* **77** 977 (2005).
- [12] R. M. Bradley, *Phys. Rev. E* **80** 061142 (2009).
- [13] L. Dagdug, I. Pineda, *J. Chem. Phys.* **137** 024107 (2012).
- [14] C. Hu, Y. Ou, J. Wu, Q. Chen, B. Ai, *J. Stat. Mech.* **2015** 05025 (2015).
- [15] H. W. Hu, L. Du, L. H. Qu, Z. L. Cao, Z. C. Deng, Y. C. Lai, *Phys. Rev. Research* **3** 033162 (2021).
- [16] J. Richardi, M. P. Pileni, J. J. Weis, *J. Chem. Phys.* **130** 124515 (2009).
- [17] Z. Yoshida, H. Saitoh, J. Morikawa, Y. Yano, S. Watanabe, Y. Ogawa, *Phys. Rev. Lett.* **104** 235004 (2010).
- [18] P. K. Ghosh, F. Marchesoni, S. E. Savelev and F. Nori, *Phys. Rev. Lett.* **104** 020601 (2010).

- [19] P. K. Ghosh, R. Glavey, F. Marchesoni, S. E. Savelev, F. Nori, *Phys. Rev. E* **84** 011109 (2011).
- [20] P. Hänggi, F. Marchesoni, S. Savelev, G. Schmid, *Phys. Rev. E* **82** 041121 (2010).
- [21] M. Sobrino Fernández, V. R. Misko, F. M. Peeters, *Phys. Rev. E* **89** 022306 (2014).
- [22] P. K. Ghosh, V. R. Misko, F. Marchesoni, F. Nori, *Phys. Rev. Lett.* **110** 268301 (2013).
- [23] Z. Liu, L. Du, W. Guo, D. C. Mei, *Eur. Phys. J. B* **89** 222 (2016).
- [24] M. Pu, H. Jiang, Z. Hou, *Soft Matter* **13** 4112 (2017).
- [25] Y. Xu, Y. Jia, M. Ge, L. Lu, L. Yang, X Zhan, *Neurocomputing* **283** 196 (2018).
- [26] B. Ai, J. Wu, *J. Chem. Phys.* **140** 094103 (2014).
- [27] S. Zhu, A. W. Yu, R. Roy, *Phys. Rev. A* **34** 4333 (1986).
- [28] X. Zhou, *Phys. Rev. A* **80** 023818 (2009).
- [29] K. Y. R. Billah, M. Shinozuka, *Phys. Rev. A* **42** 7492(1990).
- [30] S. Mondal, J. Das, B. C. Bag, F. Marchesoni, *Phys. Rev. E* **98** 012120 (2018).
- [31] R. Wittmann, J. M. Brader, A. Sharma, U. Marini Bettolo Marconi, *Phys. Rev. E* **97** 012601 (2018).
- [32] S. Mondal, B. C. Bag, *Phys. Rev. E* **91** 042145 (2015).
- [33] M. Brownnutt, M. Kumph, P. Rabl, R. Blatt, *Rev. Mod. Phys.* **87** 1419 (2015).
- [34] J. A. Sedlacek, A. Greene, J. Stuart, R. McConnell, C. D. Bruzewicz, J. M. Sage, J. Chiaverini, *Phys. Rev. A* **97** 020302R (2018).
- [35] P. K. Ghosh, *J. Chem. Phys.* **141** 061102 (2014).
- [36] B. Q. Ai, J. C. Wu, *J. Chem. Phys.* **140** 094103 (2014).